Available online at www.sciencedirect.com

ScienceDirect

IFAC PapersOnline CONFERENCE PAPER ARCHIVE

IFAC PapersOnLine 53-2 (2020) 13769–13774

Optimization of EV-Fast Charging Station Placement for Grid Support ⋆

Xiang Gao * **Sebastian Brueske** * **Markus Andresen** * and **Marco Liserre** *

* *Christian Albrechts Universitaet zu Kiel, Kiel, Germany (e-mail: xg@tf.uni-kiel.de).*

Abstract: Electric vehicle charging stations are essential for the proceeding electrification of transportation. In particular, fast charging infrastructures cause high power demands and challenge the hosting capacity of already highly loaded distribution grids. For maximizing the grid's hosting capacity, the charging infrastructure can provide grid voltage support or mitigation of current violation of devices such as transformers. Both grid support functionalities are dependent on the placement of charging stations in the grid. This work investigates the impact of charging stations' location on the potential of these functionalities. The theoretical basis of the functionalities is introduced and an algorithm for optimized placement of fast charging stations (FCS) in the grid is introduced to maximize the hosting capacity for home charging facilities (HCFs).

Keywords: Distribution networks, electric vehicles, electric vehicles charging, placement optimization, reactive power.

1. INTRODUCTION

The electrification of transportation requires suitable charging infrastructure for different users such as private or public transportation and commercial vehicle fleets, Lopes et al. (2011). Charging infrastructure for private transportation may be sufficiently served with limited power rating of residential chargers, whereas vehicle fleets require a high number of charging stations. In addition, charging management enables cost optimiziation for the purchase of charging infrastructure and the number of required vehicles, see Bin Humayd and Bhattacharya (2019). The use of electric vehicles for distances requires fast charging stations (FCS), which are absorbing high power from the grid for short times. Especially vehicle fleets and FCS require high charging power and challenge the grid's hosting capacity, even if the stochastic behavior of charging processes is considered, Calearo et al. (2019).

The grid infrastructure and the prior loading can be considered as a constraint for the installation of charging infrastructure, because grid reinforcements require significant financial investments. This applies particularly in areas with high population density and may hinder the installation of charging infrastructure. Therefore, optimal placement of EV charging stations has been proposed, Liu et al. (2013), but may still be subjected to the limited hosting capacity for charging infrastructure. An alternative to ensure safe operation of the grid is to limit the charging power or to include a pricing management in the charging process, see Hu et al. (2016). However, for extending the charging power in grids with limited hosting capacity, the charging infrastructure may provide support to the grid, see Knezovic et al. (2017); Hu et al. (2016). Voltage support in rural low voltage grids is well known and consolidated from photovoltaic applications, see Ciocia et al. (2019). Furthermore, charging infrastructure may apply power factor correction in order to reduce current violations. The potential to performing grid support depends on the location in the grid. Often, the placement has limited flexibility, and only a limited number of charging stations has flexibility in the placement.

This work investigates the impact of FCS placement in a distribution grid on the potential to perform grid support and thereby increase the EV charging station hosting capacity for home charging facilities (HCFs). The grid support by means of voltage support and limit the current through substation is applied by the FCS to maximize the installed charging power. Section 2 introduces the basics of grid congestion and Section 3 introduces the grid support functionalities in terms of voltage and current. Section 4 introduces the algorithm for placing fast charging stations and Section 5 evaluates the performance of algorithm. Finally, section 6 concludes the results.

2. GRID RESTRICTIONS AND GRID SUPPORT THROUGH FAST CHARGING STATIONS

This section introduces the grid restrictions, which are relevant with respect to an increased penetration of vehicle charging facilities. In the following, the impact of grid voltage limitations and ampacity limitations on grid devices are described along with the potential of grid-connected inverters to provide grid support.

⋆ This work was supported by the German Federal Ministry for Economic Affairs and Energy(BMWi) within Project KielFlex "Kiel als Vorbild für die Errichtung von Ladeinfrastruktur in einem flexiblen Stromnetz zur Umsetzung einer Emissionsreduktion im Transportsektor" (01MZ18002D).

10.1016/j.ifacol.2020.12.884

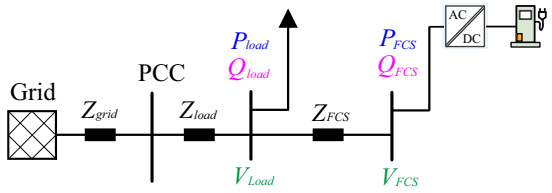

Fig. 1. Typical MV radial grid with fast charging stations.

2.1 Grid Voltage Limitations and Support

For ensuring the safe operation of the grids, the grid voltage has to be within a certain maximum deviation. As an example, the German grid code tolerates a maximum voltage deviation of 10 %. This requires to design the grid in such a way that this is guaranteed by also taking into account the active power demand P and the reactive power demand Q of the grid. Thereby, the length of the feeder along with the grid resistance R_{grid} and the grid inductance X_{grid} have a strong impact on the voltage drop ΔV with respect to the nominal grid voltage V in the grid.

$$\Delta V = \frac{R_{\text{grid}} P + X_{\text{grid}} Q}{V} \tag{1}$$

Thereby, the voltage drop ΔV is affected by variation of active power consumption P and reactive power consumption Q in the grid. Consequently, the voltage drop can be lowered by load reduction, which means limiting the charging power in case of EV charging, or by reactive power injection. In general, reactive power can be provided by passive devices such as capacitor banks or by active devices such as power electronics based, grid-connected inverters that are used in FCS. FCS can reach power ratings up to some hundred kVA, and due to charging profiles and the fact that EV chargers are not in continuous use, FCS are not full-time operated at maximum capacity to supply charging power. Therefore, the available power capacity of FCS can be used for reactive power injection and grid voltage support. In order to show the effect of reactive power injection on the grid voltage variation, a typical MV radial grid as shown in Fig. 1 is studied. The grid impedance Z_{grid} is defined by the short-circuit capacity (SCC) of the grid. The feeder supplies a load and an FCS, which are connected through the impedances Z_{FCS} and Z_{load} to the point of common coupling (PCC). The grid parameters are given in Table 1. The voltage support is implemented based on local control, for which the local voltage V_{FCS} is measured and sent to the FCS. As analyzed in Gao et al. (2017), the reactive power device farther from the substation reveals better controllability than devices close to the substation in case of radial feeders. This behavior is illustrated in Fig. 2 showing the effect of reactive power injection from −0.5 pu to 0.5 pu on the voltage V_{FCS} for different grid conditions. The comparison between Fig. 2(a) and Fig. 2(b) shows that the voltage controllability is higher in inductive grids, and the comparison between Fig. 2(a) and Fig. 2(c) illustrates that the voltage controllablity is higher in grids with lower power-voltage sensitivity. Furthermore, the gained voltage controllability is 4–5 % in the studied grid conditions.

Table 1. Parameters of MV radial grid

base voltage	10 kV
base power	1 MVA
Z_{grid}	0.01 pu
Z_{load}, Z_{FCS}	0.02 pu
$P_{\text{load}} + \text{j}Q_{\text{load}}$	(3+j0.5) pu

2.2 Current Violation Mitigation

The ampacity of a grid feeder is limited by the device with the lowest current rating, which can be either the cables or the transformers. In usual engineering practice, the transformer rating is lower than the current rating of the cables, and therefore, the current of the transformer needs to be limited. By correction of power factor, it has the potential to limit the peak current due to the reduction of reactive power flow.

In case ampacity limits are violated, the FCS can inject reactive power to reduce the imaginary part of the current. The effect of reactive power injection on the current level is shown in Fig. 3 for the same radial MV feeder and grid conditions as used in Fig. 2 with respect to the ampacitiy of line *load* in Fig. 1, which is assumed as 3.4 pu. It can be observed that for studied grid conditions, the current can be modified by the reactive power. The comparison between Fig. 3(a) and Fig. 3(b) shows that the controllability to reduce the current is not influenced by the R/X ratio, and the comparison between Fig. 3(a) and Fig. 3(c) illustrates that the controllablity is lower in grids with higher power-voltage sensitivity.

3. PLACEMENT ALGORITHM FOR FAST CHARGING STATIONS

This work proposes a placement algorithm for FCS installation. The principle of placement selection is that among groups of possible locations for installation of FCS in a grid network, the FCS at the selected locations can gain maximum controllability of the network with respect to FCS at other locations with equal power rating. The controllability is categorized into voltage support and current violation mitigation in this work. The objective functions are therefore defined as f_v and f_c. Both objectives are analyzed separately. The index EI, evaluating the performance of different locations, is defined as:

$$EI = \mu_v \cdot f_v + \mu_c \cdot f_c\,, \tag{2}$$

where μ_v and μ_c are the weights of f_v and f_c. The weights μ_v and μ_c represent the priorities assigned to voltage support and current violation mitigation. A great number of factors has an effect on the priorities, including the investment of network upgrade, the frequency of operating violations, etc. In this work, different combination of weights are analyzed to derive a systematical approach. The sum of the weights must be equal to 1:

$$\mu_v + \mu_c = 1 \tag{3}$$

The evaluation of the controllability is implemented as follows. Due to the control of FCS, extra power can be delivered to the network without violating voltage or current limits. It is assumed in this work that the extra power is fully used to supply the HCFs. The HCFs are

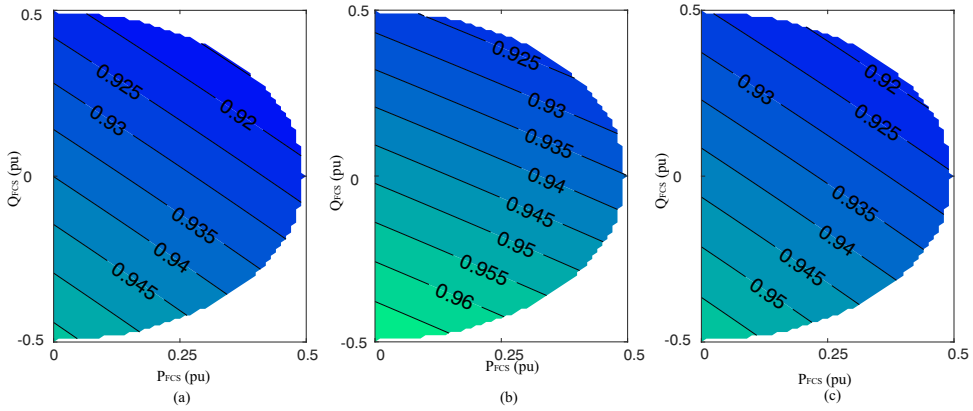

Fig. 2. Voltage level due to reactive power injection by FCS: (a) $R/X = 4:3$ and power-voltage sensitivity 1, (b) $R/X = 3:4$ and power-voltage sensitivity 1, (c) $R/X = 4:3$ and power-voltage sensitivity 2.

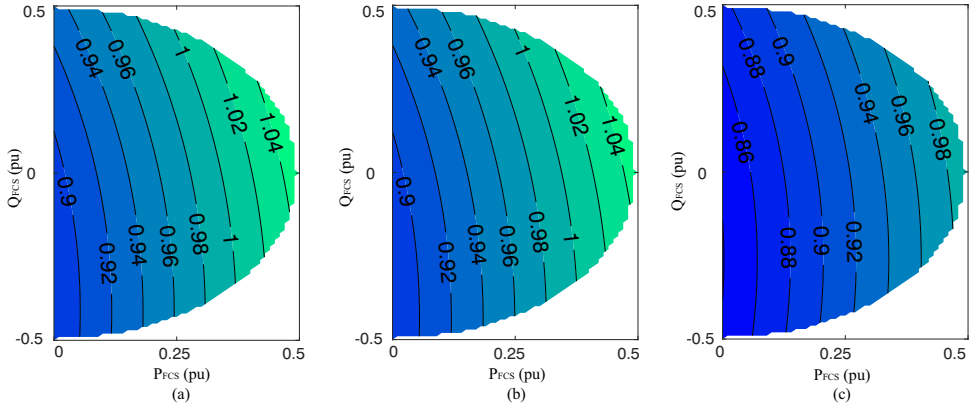

Fig. 3. Current variation due to the power change of the FCS. (a). $R/X = 4:3$, power-voltage sensitivity 1. (b). $R/X = 3:4$, power-voltage sensitivity 1. (c). $R/X = 4:3$, power-voltage sensitivity 2.

assumed to supply charging at private home with constant power and do not participate in the control. The objective function for either voltage support or current congestion management is to investigate the placement of FCS, which maximizes the permitted charging energy of HCFs. The optimization objective is defined as:

$$f = \max \int_t^T \Big(\sum_{n_p=1}^{n_{p,\max}} (p_{n_p}(t) - p'_{n_p}(t)) \cdot dt \Big) \tag{4}$$

where n_p is the node equipped with HCF, $N_p = (1, 2, ...n_{p,\max})$ is the set of nodes in the network with HCF, $p_{n_p}(t)$ and $p'_{n_p}(t)$ are the permitted charging power at node n_p of time point t with and without grid support control, respectively.

At each node n_p with HCF, it is assumed that the available number of HCF is M_{n_p}, each HCF has a constant charging power of p. The permitted charging power $p_{n_p}(t)$ can be described as:

$$p_{n_p}(t) = m_{n_p}(t)p \tag{5}$$

where $m_{n_p}(t)$ is the permitted number of HCF.

The permitted number of HCF $m_{n_p}(t)$ is assumed to be identical when $n_p \in N_p$ and must respect:

$$m_{n_p}(t) \leq M_{n_p} \tag{6}$$

To derive the optimized solutions for objective f, the constraints of power grid operation must be respected. The constraints are categorized into inequality constraints and equality constraints. The inequality constraints are imposed in the optimization, including the power rating of the FCS and operation constraints such as voltage and ampacity.

The capability of FCS reactive power injection is restricted by the power rating of FCS $S_{\text{FCS},k}$ and the charging power of EVs $P_{\text{FCS},k}$:

$$Q_{\text{FCS},k}(t) \leq \sqrt{S^2_{\text{FCS},k} - P^2_{\text{FCS},k}(t)} \tag{7}$$

where k is the node at which the FCS is connected in the network.

The voltage constraints are imposed to evaluate the voltage support f_v.

$$V_i^{\min} \leq V_i \leq V_i^{\max} \quad i \in N \tag{8}$$

The current constraints are imposed to evaluate the congestion management f_c as defined in Eq. (2). In this work, the constraint requires that the current of the substation between the grid and the main network is below the maximum allowed ampacity.

$$I_{\text{grid}} \leq I_{\text{grid}}^{\max} \tag{9}$$

The equality constraints include the power flow equations. In a network with total N nodes:

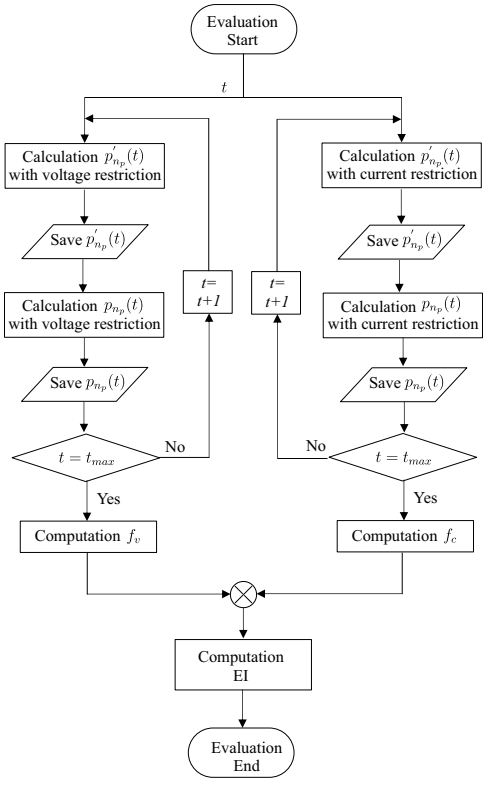

Fig. 4. The process of evaluation.

$$P_i(t) = V_i(t) \sum_{j=1}^{n_{\max}} V_j(t)[G_{ij}\cos(\delta_i - \delta_j) + B_{ij}\sin(\delta_i - \delta_j)]$$
$$Q_i(t) = V_i(t) \sum_{j=1}^{n_{\max}} V_j(t)[G_{ij}\sin(\delta_i - \delta_j) - B_{ij}\cos(\delta_i - \delta_j)] \quad (10)$$

where $i \in N$ and $N = (1...n_{\max})$ is the set of nodes in the network. $P_i(t)$ and $Q_i(t)$ are active and reactive power demand at node i, respectively. It is the aggregated load, which represents all devices connected to i, e.g. the charging power of $p_{n_p}(t)$ is considered within $P_i(t)$ when $i \in N_p$ ($N_p \subseteq N$). G_{ij} and B_{ij} are transfer conductance and susceptance between node i and j.

By injecting reactive power into the grid, also the grid voltage profile is affected. Remarkably, the power consumption of the loads may be affected, which is referred to as the power sensitivity to voltage, and is defined as:

$$P_i(t) = P_{i0}\left(V_i(t)/V_{i0}\right)^{k_{pi}}$$
$$Q_i(t) = Q_{i0}\left(V_i(t)/V_{i0}\right)^{k_{qi}} \quad (11)$$

Thereby, k_{pi} and k_{qi} are the power voltage sensitivities, P_{i0}, Q_{i0} and V_{i0} are the respective power and voltage references, $P_i(t)$, $Q_i(t)$ and $V_i(t)$ are the real time power and voltage, respectively.

The diagram of the evaluation process is represented in Fig. 4.

4. EVALUATION OF PLACEMENT ALGORITHMS

The algorithm is analyzed by means of simulation in a testing network with scenarios of different locations to install FCS.

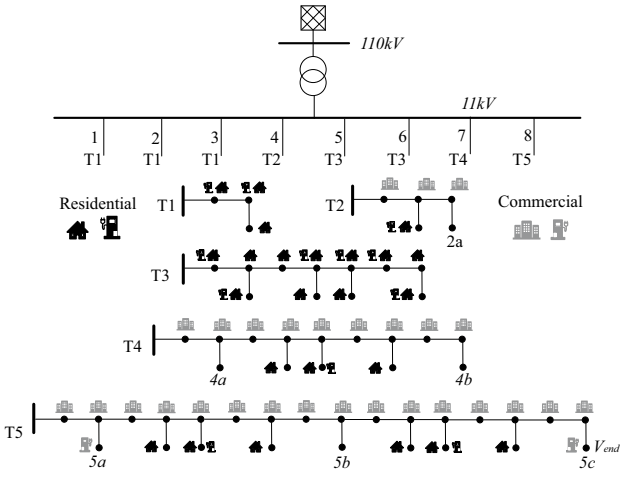

Fig. 5. The structure of testing network.

4.1 Operation Condition of Testing Netwrok

A testing network based on the UK distribution benchgrid is modeled for simulation. A substation connects the testing network to the main grid of upper voltage level. The short circuit capacity of the main grid is assumed to be 500 MVA. The substation has a power capacity of 52.8 MVA. Eight radial feeders are modeled. The feeders have the voltage level of 11 kV. As shown in Fig. 5, the network consists of 75 different loads, including residential/commercial areas, the FCS and HCFs. The base power is 1 MVA.

The base power of a residential load without HCF and commercial load is (0.45+j0.1) MVA and (0.6+j0.25) MVA, respectively. The power rating of the commercial FCS is 0.6 MVA. At the nodes, where the HCFs are connected, the base power of a load is (0.35+j0.1) MVA. Each node is equipped with 10 HCFs, and each HCF can provide a constant charging power of 10 kW. The loads and the commercial FCS follow the corresponding 24 h power profiles presented in Fig. 6. The power-voltage sensitivities are listed in Table 2.

The analysis is based on the assumption that four FCS must be installed, for which six possible locations are available. The goal is to identify the locations, which maximizes the hosting capacity of HCSs in the entire grid. In total 15 scenarios arise for the analysis, listed in Table 3. For each scenario, four locations are selected to install one FCS per location.

4.2 Placement for Voltage Support

The performance of different scenarios with respect to the voltage support has been analyzed. The objective of the control is to maintain the voltage of the complete grid within 0.9–1.1 pu, while the penetration of HCF increases. The f_v represents the increment of HCF charging energy of a duration of 24 h. The results are listed in Table 4 according to Table 3. It can be observed that the f_v of scenarios S10, S14 and S15 have the maximal results of the same value. For all three scenarios, there are three FCS in feeder 8, which has a lower R/X ratio. The result of S1 has the lowest value. It can be concluded that the voltage

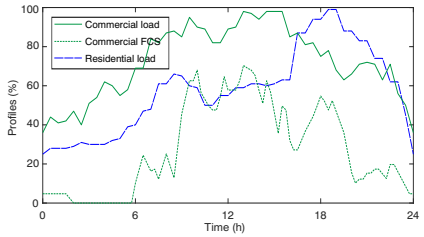

Fig. 6. The 24 h profiles for load and FCS.

Table 2. Sensitivity of power-voltage (pu)

Sensitivity	k_p	k_q
Residential	1.25	2.75
Commercial	1.25	1.75

Table 3. Scenarios of placement

Scenario	Selected nodes	Scenario	Selected nodes
S1	2a, 4a, 4b, 5a	S2	2a, 4a, 4b, 5b
S3	2a, 4a, 4b, 5c	S4	2a, 4a, 5a, 5b
S5	2a, 4a, 5a, 5c	S6	2a, 4a, 5b, 5c
S7	2a, 4b, 5a, 5b	S8	2a, 4b, 5a, 5c
S9	2a, 4b, 5b, 5c	S10	2a, 5a, 5b, 5c
S11	4a, 4b, 5a, 5b	S12	4a, 4b, 5a, 5c
S13	4a, 4b, 5b, 5c	S14	4a, 5a, 5b, 5c
S15	4b, 5a, 5b, 5c		

Table 4. Increment of HCF charging energy f_v (MWh)

Scenario	f_v	Scenario	f_v	Scenario	f_v
S1	5.50	S2	6.75	S3	8.75
S4	7.25	S5	9.20	S6	10.95
S7	7.25	S8	9.20	S9	10.95
S10	11.50	S11	7.25	S12	9.20
S13	10.95	S14	11.50	S15	11.50

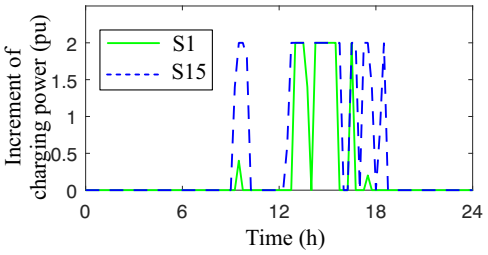

Fig. 7. 24 h increment of HCF charging power derived from f_v.

support is more effective, if the FCS are installed at the locations of scenarios S10, S14 and S15.

The 24 h profiles of charging power increment $p_{n_p}(t) - p'_{n_p}(t)$ are shown in Fig. 7. It can be clearly observed that around 10:00 and between 16:00-19:00, the charging power of S15 has been significantly increased in respect to S1. The maximal power difference of the two scenarios is 2 pu. The maximal available charging power for HCFs is increased by around 7 % of the load power of entire network, which is approx. 30 pu. The charging energy available for HCFs without and with control is 42.50 MWh and 48.00 MWh in S1, and 36.50 MWh and 48.00 MWh in S15. This corresponds to an increase of 12.9 % and 31.5 %, respectively. The 24 h voltage profiles at node 5c are shown in Fig. 8. Based on the authors' knowledge, this node has

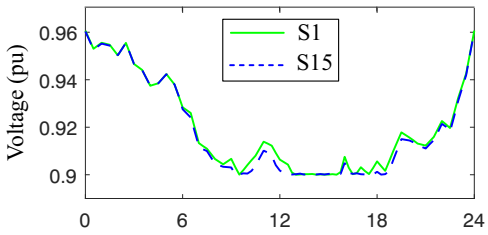

Fig. 8. 24 h voltage profiles derived from f_v.

Table 5. Increase charging energy f_c (MWh)

Scenario	f_c	Scenario	f_c	Scenario	f_c
S1	1.85	S2	1.85	S3	1.85
S4	1.90	S5	1.90	S6	1.85
S7	1.85	S8	1.90	S9	1.90
S10	1.90	S11	1.85	S12	1.85
S13	1.90	S14	1.90	S15	1.90

the largest electrical distance to the substation, which has the maximal voltage deviation. It is noted that the voltage of both scenarios has been maintained above 0.9 pu.

4.3 Placement for Current Congestion Management

The performance of current congestion management implemented with different scenarios has been analyzed. It is assumed that the current should be limited to $I_{\max}$ equal to 30 pu. The increment of charging energy f_c of a duration of 24 h is presented in Table 5 based on scenarios in Table 3. It can be observed that the results of f_c. have two values. The higher value is 1.90 MWh, which is 0.05 MWh higher than the other value. The difference is not significant. The results of f_c of the scenarios S10, S14 and S15 have the same value of 1.90 MWh. The value of f_c is 1.85 MWh of S1.

The 24 h profiles of charging power increment $p_{n_p}(t) - p'_{n_p}(t)$ are shown in Fig. 9. It can be observed that the difference of the charging power is very small between the two scenarios. The increment is also less than 0.8 pu. The charging energy for HCFs without and with control is 41.15 MWh and 43.00 MWh with S1 and 41.00 MWh and 42.90 MWh with S15. The increases are 4.3 % and 4.6 % respectively.

The 24 h profiles of the substation current are shown in Fig. 10. The current of both scenarios has been restricted no more than $I_{\max}$.

4.4 Evaluation of Placement Scenarios

The placement scenarios are evaluated with index derived from Eq. (2). The optimal scenario should have the highest index. The results of optimization functions f_v and f_c have been derived. It is noticed that the results of f_v are considerable higher than the results of f_c. The minimum difference is approx 3 times higher. The mitigation current violation can be however more important than the voltage support. Therefore, proper weights μ are required to achieve plausible results. On the other hand, the index μ varies with the network operation conditions and can be completely opposite from case to case. In order to have a systematical analysis, different weights are selected to compute the value of index EI from Eq. (2). The indices

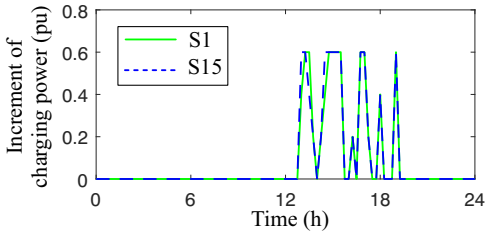

Fig. 9. 24 h increment of HCF charging power derived from f_c.

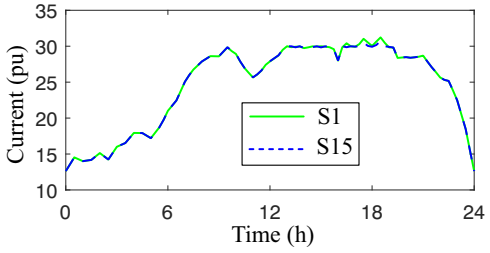

Fig. 10. 24 h current profiles derived from f_c.

Table 6. Indices EI of selected scenarios of different (μ_v,μ_c)

Scenario	(0.95,0.05)	(0.8,0.2)	(0.2,0.8)	(0.05,0.95)
S1	5.32	4.77	2.58	2.03
S5	8.84	7.74	3.36	2.26
S6	10.50	9.13	3.67	2.31
S6	10.50	9.14	3.71	2.35
S15	11.02	9.58	3.82	2.38

of five scenarios are listed in Table 6 according to different values of (μ_v,μ_c).

The results of indices show that for all selected weights, the index of S15 has the highest value and the indes of S1 has the lowest value. The four FCS should be installed to the nodes, which are considered in S15, for instance. However, the difference has been reduced from 51.7 % (when f_v is dominated) to 14.7 % (when f_c is dominated). By comparing the index of S5 and S6, it is noticed that when the weight μ_c increases, it is possible that the index of S5 becomes higher than that of S6, which eventually changes the decision of FCS placement. It is therefore concluded that the appropriate weights are essential for identification of optimal FCS placement. The weights must be individually adjusted based on the network condition.

5. CONCLUSIONS

This paper proposes an optimal placement algorithm for fast charging stations based on multi-objective optimization of grid operation. Free power capacity can be used for grid support by reactive power injection, and the algorithm evaluates the achievable grid controllability to increase the grid's hosting capacity for home charge facilities. A case study based on the UK distribution benchgrid has been carried out by simulation, and the potential of voltage support and current violation mitigation to increase the maximum charging power of home charging facilities has been investigated. The results show that voltage support increases the charging energy by 12.9–31.5 % in a 24 h duration. Using reactive power for current violation mitigation, the maximum charging power can be increased by 4.3–4.6 % in a 24 h duration. Weights are introduced to evaluate optimal locations considering all possible grid support functions. The results confirm that higher controllability can be gained with fast charging stations at proper locations.

REFERENCES

Bin Humayd, A.S. and Bhattacharya, K. (2019). Design of optimal incentives for smart charging considering utility-customer interactions and distribution systems impact. *IEEE Transactions on Smart Grid*, 10(2), 1521–1531. doi:10.1109/TSG.2017.2771508.

Calearo, L., Thingvad, A., Suzuki, K., and Marinelli, M. (2019). Grid loading due to ev charging profiles based on pseudo-real driving pattern and user behavior. *IEEE Transactions on Transportation Electrification*, 5(3), 683–694. doi:10.1109/TTE.2019.2921854.

Ciocia, A., Boicea, V.A., Chicco, G., Di Leo, P., Mazza, A., Pons, E., Spertino, F., and Hadj-Said, N. (2019). Voltage control in low-voltage grids using distributed photovoltaic converters and centralized devices. *IEEE Transactions on Industry Applications*, 55(1), 225–237. doi:10.1109/TIA.2018.2869104.

Gao, X., De Carne, G., Liserre, M., and Vournas, C. (2017). Voltage control by means of smart transformer in medium voltage feeder with distribution generation. In *2017 IEEE Manchester PowerTech*.

Hu, J., Si, C., Lind, M., and Yu, R. (2016). Preventing distribution grid congestion by integrating indirect control in a hierarchical electric vehicles' management system. *IEEE Trans. Transport. Electrific.*, 2(3), 290–299. doi: 10.1109/TTE.2016.2554469.

Hu, J., Morais, H., Sousa, T., and Lind, M. (2016). Electric vehicle fleet management in smart grids: A review of services, optimization and control aspects. *Renewable Sustainable Energy Rev*, 56, 1207–1226.

Knezovic, K., Martinenas, S., Andersen, P.B., Zecchino, A., and Marinelli, M. (2017). Enhancing the role of electric vehicles in the power grid: Field validation of multiple ancillary services. *IEEE Transactions on Transportation Electrification*, 3(1), 201–209. doi: 10.1109/TTE.2016.2616864.

Liu, Z., Wen, F., and Ledwich, G. (2013). Optimal planning of electric-vehicle charging stations in distribution systems. *IEEE Transactions on Power Delivery*, 28(1), 102–110. doi:10.1109/TPWRD.2012.2223489.

Lopes, J.A.P., Soares, F.J., and Almeida, P.M.R. (2011). Integration of electric vehicles in the electric power system. *Proceedings of the IEEE*, 99(1), 168–183. doi: 10.1109/JPROC.2010.2066250.